ORIGINAL ARTICLE

Study on the regulation of deformation uniformity and microstructure law in the forming of gear shafts by cross wedge rolling

Chen Lulu[1] · Shu Xuedao[1] · Chen Xiaogu[1] · Gong Wenwei[1] · Li Zixuan[1] · Xu Haijie[1]

Abstract

Gear shafts are commonly manufactured by machining of gear teeth and shaft separately. This kind of approach entails quite some problems, such as long processing time, large die, and low production efficiency. To tackle these problems, this paper innovatively proposes a new process of cross wedge rolling (CWR) that is specifically tailored to the manufacturing of gear shafts, with which the shaft and teeth are formed at one go. The finite element model of CWR forming of gear shaft is established to simulate and analyze the CWR forming process. A three-factor and three-level response surface test is designed to optimize the processing parameters, where the friction coefficient, rolling temperature, and die movement speed are chosen as three factors, and inhomogeneous deformation is set as the response. The optimal parameters are obtained as follows: the rolling temperature is 1240 ℃, the speed of the die movement is 336 mm/s, and the friction coefficient is 0.8. This result is subsequently verified by experiments. Further on, the microstructure evolution of the characteristic points of the CWR forming process of gear shaft is analyzed. It is found that the grains at the gear teeth section are continuously refined and grown from the boundary at the early section of deformation, and the final grains grown are much smaller than the original ones. In addition, the grains appear to grow in a short range of time in the process of deformation, but the overall trend is towards refinement. In the shaft section, the evolutions of the grains in the two stepped shaft segments are almost the same; the grain deformation shows cyclic changes; the degree of grain refinement in the shaft is higher than that in the teeth; and the degree of grain refinement in the shaft center is higher than that in the shaft edge. The results of the study provide a theoretical basis for short-process forming of high-performance gear shafts by cross wedge rolling.

1 Introduction

Cross wedge rolling (CWR) [1] exhibits high productivity and high material utilization as compared with conventional machining processes. It is an advanced method for producing long shaft parts and stepped axles as well as preforms for die forging, and the development has become mature [2, 3]. Gear shafts are stepped shafts with gears, and are key components of the transmission system in mechanical equipment. The deformation in the manufacturing of gear shafts is larger and more complex than those in ordinary stepped shafts and hollow shafts with the conventional manufacturing techniques [4, 5]. How to realize high-performance manufacturing of gear shafts is a cutting-edge topic. Scholars from different countries have carried out researches from various perspectives.

For the precision forming of shafts with CWR technology, a lot of research has been carried out to improve the quality of CWR shaft parts [6]. Pater et al. used the finite element method (FEM) to analyze 54 cases in CWR, and they make it possible to predict material fracture in CWR with great accuracy [7, 8]. In order to solve the concave center at the end of the formed shaft in CWR process and to improve the quality of the shaft, Zeng used the element simulation software to simulate the forming process of a large number of rolling work pieces. The quadratic orthogonal rotation combination was used to explore the influence of process parameters on the depth of the concavity under the flat face. The study results showed that the concavity is

✉ Shu Xuedao
  shuxuedao@nbu.edu.cn

  Chen Lulu
  2211090080@nbu.edu.cn

[1] College of Mechanical Engineering and Mechanics, Ningbo University, Ningbo 315211, China

in direct proportion to the cone angle, but in inverse proportion to the central angle [9]. Han et al. conducted statistical analysis through statistical product and service solutions software to obtain the minimum depth of the concave center within the allowable range of process parameters [10]. Qu et al. analyzed the forming process and metal flow law of stepped hollow shaft. Taking the relationship between radial reduction and inner hole diameter change after rolling as the object, they studied the influence of original relative wall thickness and rolling temperature on the relationship, using MATLAB to fit the variation law of radial reduction and inner hole diameter under different section shrinkage during the rolling process of stepped hollow shaft, and obtained a unified fitting formula above 50% shrinkage [11]. Yan et al. obtained the law for the variation of wall thickness by means of FEM and experiment. The results confirmed that when a hollow valve with a mandrel is formed with the CWR process, there was a critical diameter of the mandrel. It made wall thickness of the hollow valve optimal [12]. In recent years, the internal microstructure of CWR shaft parts has attracted more and more attention [13, 14]. Xia et al. analyzed the effect of process parameters on microscopic uniformity of CWR of GH4169 alloy shaft, and obtained the optimal process parameters [15]. Xu et al. studied the effects of three important process parameters, rolling temperature, rolling speed, and reduction of area, on the evolution of microstructure basing on the cellular automata model, through metallographic experiments, and they concluded that in the β single-phase region, the grain size of the rolled piece increases with the increase of rolling temperature, and decreases with the increase of rolling speed and section shrinkage [16].

For the forming of gear teeth in gear shafts, Chen et al. adopted the single-factor research method to carry out the most appropriate feed rate. The results show that the total rate is 2.75 mm and the suitable range of the feed rate in the first section is 1.0–1.2 mm [17]. Xu et al. used DEFORM-3D finite element software to simulate the forming process of involute spur gear shaft by CWR; plastic equivalent strain, rolling force, and gear forming effect were acquired [18]. Subsequently, the causes of the phenomenon of tooth defects and chaotic teeth of involute gear shafts during plate cross wedge rolling experiments or actual production were analyzed, which could appear at the initial section of rolling and in the middle and late sections of the formation of the tooth profile [19]. Cai et al. studied the influence rule of billet temperature on the tooth profile rolling precision of

involute spur gear shaft cross wedge rolling; the simulation results showed that with the increase of the temperature of the metal tooth blank, the first section of the die pitch cannot be correctly divided and must be corrected [20]. Merkel et al. investigated an innovative process chain for the production of hybrid components. A near-net shape geometry was achieved for the pinions made of steel [21].

In summary, the existing research on gear shaft forming is mainly focused on the approach by manufacturing the teeth part and the shaft part separately. The research on integrated forming of both shaft and teeth is rare, and there is little research on the forming quality and the non-uniformity of the finished product. Experimental validation is also lacking, due to which the forming quality of the blank is still based on the observation method, and there is no experimental validation based on microscopic grain. Therefore, this paper carries out a study on the uniformity of integrated forming of gear shafts by cross wedge rolling, which is of great significance.

2 Finite element model and simulation parameters

2.1 Constitutive model

The Johnson–Cook (J-C) model has been widely used in the description of the dynamic properties of ductile metallic materials because of its simple form, clear physical meaning, and easily accessible parameters. The model of 45 steel used in this research refers to article [22], and the constitutive model formula is shown below:

$$\sigma_{eq} = \left(A + B\varepsilon_{eq}^n \right)\left[1 + C\ln\left(\dot{\varepsilon}_{eq}^* \right) \right]\left(1 - T^{*m} \right) \tag{1}$$

where A is the yield strength of the material at the reference strain rate and reference temperature, B and n are the strain intensification factors, C is the strain rate sensitivity factor, m is the temperature softening factor, and σ_{eq} is the equivalent stress; ε_{eq} is the equivalent plastic strain, $\dot{\varepsilon}_{eq}^*$ is the dimensionless equivalent plastic strain rate, $\dot{\varepsilon}_{eq}^* = \dot{\varepsilon}_{eq}/\dot{\varepsilon}_0$, and $\dot{\varepsilon}_0$ is the reference strain rate; T^* is the dimensionless quantized temperature, $T^* = (T - T_r)/(T_m - T_r)$ where T_r and T_m are the reference temperature (293 K) and the melting point of the material (1513 K), respectively, and T is the current temperature. The specific parameters in the equation are shown in Table 1.

Table 1 Parameters of the intrinsic model for 45 steel J-C

E/GPa	ν	ρ/(kg•m^3)	C_p/(J·(kg·K)$^{-1}$)	T_r/K	T_m/K	m	A/MPa	B	n	$\dot{\varepsilon}_0$/(s^{-1})	C	W_{cr}/MPa
210	0.33	7850	469	293	1513	0.698	714	563	0.518	8.33×10^{-4}	0.037	547

2.2 Establishment of finite element model

This paper takes the gear shaft as the research object, which was shown in Fig. 1, where the gear shaft length is 140 mm, the diameters of two stepped shaft segments are 25 mm and 29 mm, respectively, and the gear module is 2 mm, with the number of teeth being 18. According to the principle of equal volume, the blank diameter of 37.5 mm can be derived.

By using rolling rather than the conventional material-removal machining for the manufacturing of gear teeth, a toothed die will be employed rather than the conventional cutter gear, which is constructed by four sections of gear teeth. The parameters of the die are shown in Fig. 2. In the rolling section, too small feed of the toothed die will lead to the formation of the gear being not full enough, while too large feed will lead to metal spillage in the rolling process of the gear, thus unable to form the gear. Because the toothed die bites into the blank work, with which the root work of the gear teeth is formed, the total height from the die biting is 2.5 mm, which means, it is 2.5 mm initially. Besides, in order to ensure the smooth progress of the rolling process, there should be 0.25 mm space between the top of the die contour and the root of the gear to be formed, hence is set to 2.75 mm finally. During cross wedge rolling of gears, the main deformation is in the early section, with small feed being reserved at the later sections for correction and adjustment purposes. As such, the die gear heights at the four sections are 2.75 mm, 3.4 mm, 4.0 mm, and 4.5 mm, respectively. When the pitch circle of the tooth shape of the blank has been processed, the transmission relationship between the die gear and the blank gear shall be close to the mesh relationship. As a result. when the cumulative increase in the amount of feed is greater than the height of the top of the finished gear teeth, the tooth pitch can be considered no longer changing. Therefore, we should set the tooth pitch of the die gear in the first phase to be slightly larger than the standard tooth pitch. Due to the fact that the tooth pitch difference between the first phase and the second phase is large, which will lead to the position of the die biting into the blank be deviated at the second phase, so the tooth pitch of the die should be assigned with an intermediate value between the first phase and the second phase, such that the die biting can be made more stable into the position of the blank. After calculation, the tooth pitch of the die in the first section is 6.54 mm, while that between the first and second section is 6.41 mm, and it is 6.28 mm for the remaining sections.

In summary, the cross wedge rolling model for the forming of gear shaft is established, as shown in Fig. 3. The model mainly includes a pair of toothed dies, i.e., the upper die and lower die, the blanks, and the baffles. The upper and lower dies are identical, symmetrically positioned in the center, and move in opposite directions in a uniform linear motion during the process. At
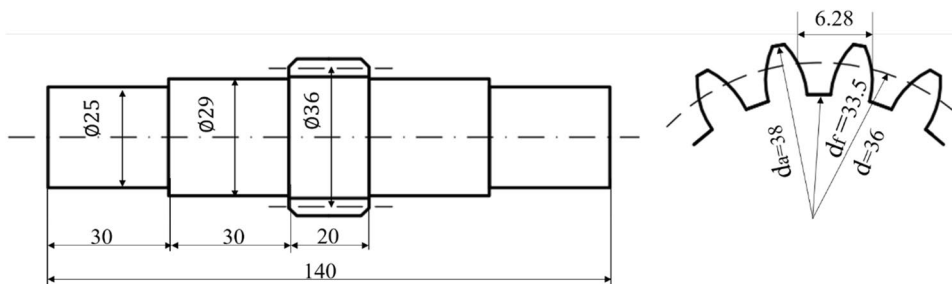
Fig. 1 Gear shaft drawing

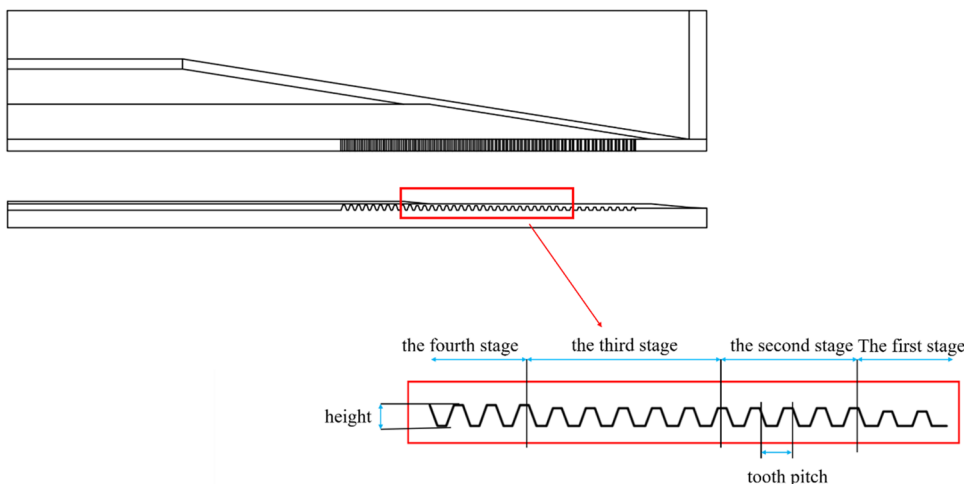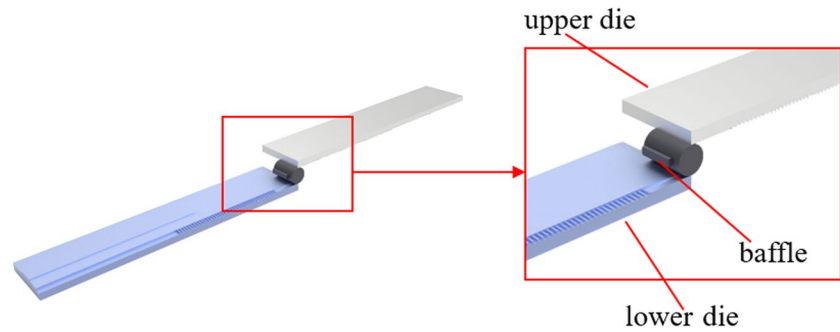**Fig. 2** Geometric parameters of the toothed die

Fig. 3 Cross wedge rolling model for the forming of gear shaft

the beginning of the rolling process, the blank will be compressed to the required size in the wedge-shaped die wedge section, and then in the spreading section of the synchronous rolling of the gear and stepped shafts. Both the toothed dies and the wedge-shaped section of the dies are designed with the ending section to be used as the finial finishing of the product, so as to ensure that the quality of the finished product. The geometric parameters of the upper and lower dies are shown in Fig. 4. The wedge angle is $\alpha = 30°$, the spreading angle is $\beta = 9°$, the first wedge height H_1 is 3 mm and second H_2 is 2 mm, the wedge length of the first stepped shaft L_1 is 32.8 mm, the spreading length of the section L_2 is 160 mm, the wedge length of the second stepped shaft L_3 is 21.9 mm, the spreading length of the section L_4 is 69 mm, and the finishing length L_5 is 49 mm.

2.3 Setting of simulation parameters

In order to ease the study, the model needs to be simplified as follows during the full process of the restricted element simulation:

(1) The die is regarded as a rigid body that cannot be deformed.
(2) The rolled work is a plastic body, ignoring its elastic deformation.
(3) Neglect the heat exchange between the die, the roll, and the air.
(4) The gear axis is completely symmetric, so only half of the model is used for the finite element simulation to reduce the computational cost.

The finite element simulation parameters are set as listed in Table 2, where the simulation steps shall be kept on until when the rolled work is to its full accomplishment.

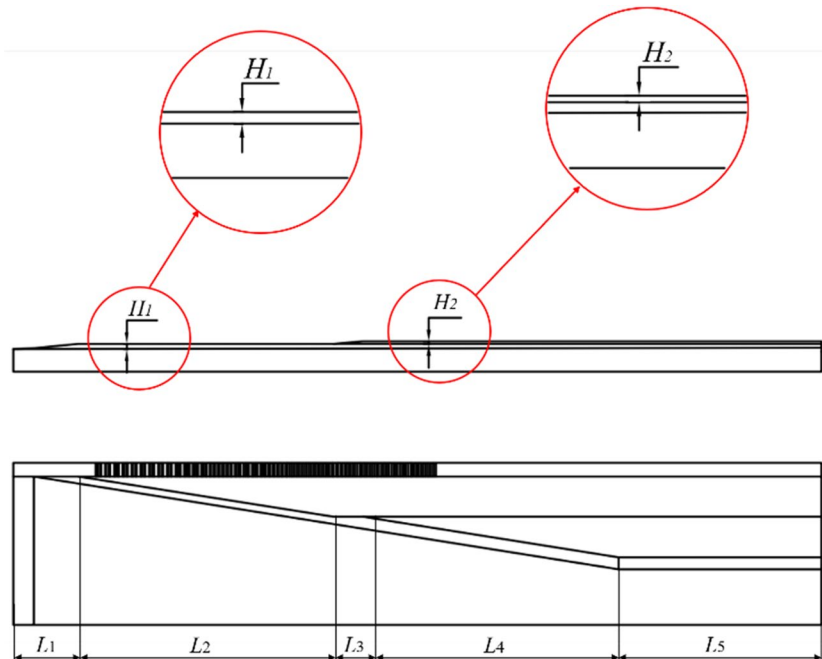**Fig. 4** Geometric parameters of the upper and lower dies

Table 2 Finite element simulation parameters

Parameters	Numbers
Material	45 steel
Blank preheating temperature	1000–1300 ℃
Ambient temperature	20 ℃
Movement speed	50–350 mm/s
Friction between die and rolled work	− 1.2

3 The cross wedge rolling process of gear shaft

3.1 Forming process

The proposed forming process of gear shaft by cross wedge rolling integrates the CWR technology and the gear generating principle, so that the stepped shaft and gear can be formed at one go, as shown in Fig. 5. It goes from the rolling of shaft alone, to the integrated rolling of shaft and gear, and finally the rolling of shaft alone again. The entire process can be detailed as consisting of five phases or sections, as shown in Fig. 5a.

From the perspective of change in feed, the forming process can also be divided into three stages, i.e., the splitting-into-teeth section, the forming stage, and the final finishing section, as shown in Fig. 5b. During the splitting stage, the tooth top of the die and the outer edge of blank come into contact; thus, the root work of the work makes the first deformation. In this stage, the die biting is shallow and the focus of the process is to make an accurate bite and ensure accurate teeth splitting. During the forming section, the amount of plastic deformation of the blank gradually increases, and the involute teeth profile is gradually formulated. In the finishing section, the die feed remains constant, indicating no further feeding or compressing. Consequently, the gear shape is essentially defined. Besides, the die continues to move to make the final finishing of the teeth.

3.2 Strain field distribution

The equivalent strain distribution of the gear cross wedge rolling process is shown in Fig. 6. Figure 6a shows that the strain is mainly concentrated in the contact area between the die and the rolled work, and the maximum equivalent strain reaches 3. The strain gradually decreases from the contact area to the end of the axis, forming a similar elliptical stress concentration area; this means that the strain is mainly caused by the rotation of the rolling work, which is carried by the die. As can be seen from the profile, the internal strains are

Fig. 5 Sections of the forming process of gear shaft. **a** Five sections of rolling. **b** Three sections with respect to feed change

(a)

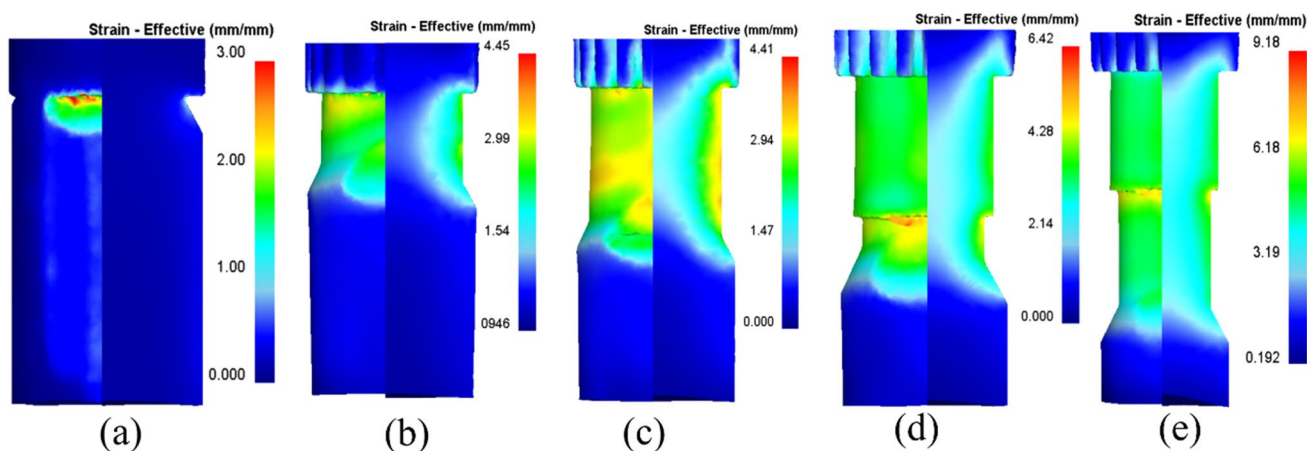teeth dividing stage   forming stage   finishing stage

（b）
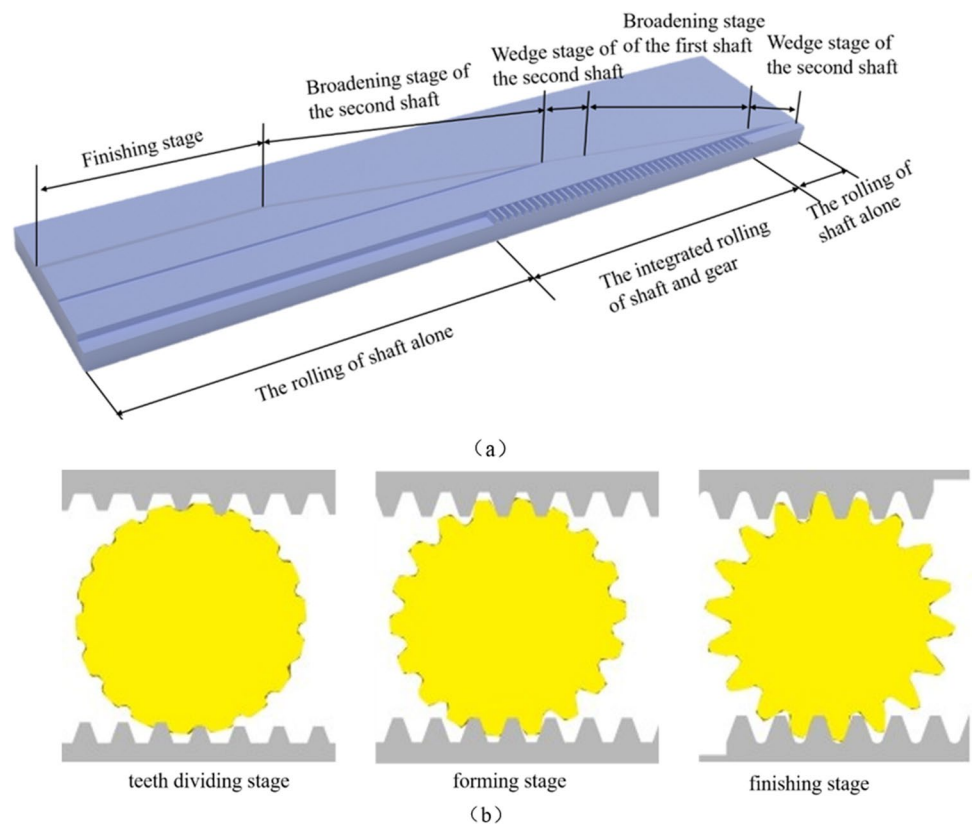
Fig. 6 Distribution of equivalent strain during cross wedge rolling of gear. **a** First wedge entry section. **b** First widening section. **c** Second wedge entry section. **d** Second widening section. **e** Finishing section

relatively small, from the stress concentration area along the radial direction shows a decreasing trend, this is due to the rolling works and die direct contact area faster, extrusion of metal to form a large strain zone, the internal metal deformation rate is weaker, and gradually to the middle of the decreasing to 0. In Fig. 6b, the die and blank contact area, the maximum equivalent strain increased to 4.45, and the minimum equivalent strain from 0 to 0.0946; this indicates that the gear shaft has deformed on all axes under the drive of the die. In the widening section, due to the larger contact area between the die and the blank, the overall stress concentration area expands, leading to a flattening trend in the strain change. Additionally, the profile indicates a decreasing trend in strain along the radial direction (Fig. 6c). The equivalent strain area of the gear work is mainly concentrated in the tooth's profile, and this proves that the forming of the teethed part is mainly done by extruding the metal at the tooth's root to fill the metal at the teeth's top. The area of equivalent strain distribution at the shaft is similar to that of the first spreading section because the die in the first spreading section still has a finishing contact on the shaft. In the wedge portion of the die, there is a strain concentration area similar to the first wedge portion, and the cause is the same as that of the first wedge portion (Fig. 6d). The maximum equivalent strain increases to 6.42. The equivalent strains at the rest of the locations and their causes are the same as those in the first spreading stage. In Fig. 6e, the maximum equivalent strain reaches 9.18. Upon completion of the gear shaft tooth machining, the tooth deformation area diminishes to zero, indicating a tendency for shaft deformation to propagate to both sides. Throughout the shaft body, the equivalent strain area remains uniform.

4 Uniform deformation of gear shaft by cross rolling forming

4.1 Test program design and analysis based on the BBD method

Rolling temperature directly affects the plastic deformation of the rolled work, which is one of the important factors to make the rolled work become elliptical. Die movement velocity and friction are important causes of gear shaft's slip phenomenon. The improper parameters will seriously affect the rolling process and even lead to rolling rotating difficulties. Therefore, in this paper, the die movement velocity, friction coefficient and rolling temperature are selected as three factors, and the uniformity of deformation is taken as the response of each parameter, and the response surface test of three levels and three factors is designed by Box-Behnken design method.

According to reference [23], the range of the three factors involved in the fitting design was obtained, and the designed test factors and their levels were shown in Table 3.

There isn't a single set of data that can definitively indicate whether deformation is uniform across a system or not. Therefore, it is necessary to quantify the deformation in order to study

Table 3 Box-Behnken design test factors and levels table

Level	A—Temperature	B—Velocity	C—Friction coefficient
−1	1000	50	0.8
0	1200	200	0.9
1	1300	350	1.0

the relationship of each parameter to the deformation uniformity, and the quantitative expression is shown in Eq. (2).

$$R = \frac{\varepsilon_{\max} - \overline{\varepsilon}}{\overline{\varepsilon}} \tag{2}$$

where R is a quantitative indicator of the uniformity of deformation, that is, the response; $\varepsilon_{\max}$ is the maximum strain value; $\overline{\varepsilon}$ is the average strain; the smaller the value of R, the higher the uniformity of the rolled works; the larger the value of R, the lower the uniformity of the rolled works after rolling.

In this paper, a three-factor test is designed based on the Box-Behnken design (BBD) method, requiring the testing of 13 groups of data. These 13 test scenarios for simulation and simulation results are processed to obtain quantitative values of deformation uniformity (R-value). The data in Table 4 were input into the Design-Expert for function fitting of parameters and R-values; in terms

Table 4 Quantitative values of inhomogeneous deformation

Group number	A	B	C	R
1	− 1	− 1	0	14.99
2	1	− 1	0	14.70
3	− 1	1	0	11.19
4	1	1	0	11.11
5	− 1	0	− 1	14.47
6	1	0	− 1	16.24
7	− 1	0	1	16.56
8	1	0	1	15.14
9	0	− 1	− 1	14.22
10	0	1	− 1	11.00
11	0	− 1	1	15.90
12	0	1	1	12.09
13	0	0	0	12.52

of the response to the R, the second-order model has the best fitting effect.

4.2 Effect of process parameters on inhomogeneous deformation

In the response surface method, the interaction between two parameters and the relationship with the response can be revealed by the three-dimensional interaction diagram and contour plot between the two parameters. The steeper the surface in the three-dimensional plot and the denser the contour lines in the contour plot, the more significant the effect of the parameters. In this paper, in order to obtain the smallest inhomogeneous deformation, the optimum value is at the lowest point of the surface in the three-dimensional plot, and the optimum value is at the center of the ellipse in the contour plot (contour lines shown in ellipse indicate a significant interaction, and contour lines shown in circle indicate a non-significant interaction).

The interaction between temperature and die velocity is shown in Fig. 7. The contour plot of Fig. 7b shows an ellipse-like shape, so the interaction between temperature and die velocity is obvious. It can be seen from Fig. 7a that at the left position in 3D space, the inhomogeneous deformation reaches a minimum value, and at the top right position in the figure, the inhomogeneous deformation reaches a maximum value. It can be seen from Fig. 7b that the contour lines are most densely located in the top right and bottom left corners, which indicates that when the temperature is certain, the inhomogeneous deformation increases with the velocity of the die. The effect becomes more pronounced as the velocity approaches 350 mm/s; when the die velocity is certain, the inhomogeneous deformation becomes smaller and then larger; the degree of inhomogeneous deformation decreases as the temperature approaches 1100 °C. Combining Fig. 7a and b, it can be concluded that in the temperature range of

Fig. 7 Interaction between temperature and die velocity. **a** Three-dimensional plot of temperature–velocity interaction. **b** Contour plot of temperature–velocity interaction

1050–1150 ℃, the velocity in the range of 300–350 mm/s inhomogeneous deformation is smaller.

The interaction between temperature and friction coefficient is shown in Fig. 8. The contour plot in Fig. 8b clearly exhibits a standard ellipse shape, so the interaction between temperature and friction coefficient die velocity is obvious. Figure 8a is a concave surface. In the three-dimensional space depicted in the figure, it is observed that the inhomogeneous deformation reaches its minimum at the center. Here, the friction coefficient is set to 0.8, and the temperature is close to 1100 ℃. The inhomogeneous deformation gradually increases in all directions from the center of the space to the surroundings, and it reaches a maximum at the junction of the critical values of the temperature and the friction coefficient. The contour lines of Fig. 8b show a concentric ellipse shape, and the farther away from the center ellipse contour lines are denser. This suggests that the inhomogeneous exhibits a negligible trend with the variation of the two factors once the temperature and friction coefficient reach a certain value. While the temperature is certain, the inhomogeneous deformation with the increase of the friction

coefficient firstly becomes larger, then smaller, and finally larger; while when the friction coefficient is certain, the inhomogeneous deformation with the increase of the temperature firstly becomes larger and then smaller. Combining Fig. 8a and b, it can be concluded that the temperature is in the range of 1050–1150 ℃, the coefficient of friction in the vicinity of 0.8 is the best effect, and the inhomogeneous deformation can reach a smaller value.

The interaction between die velocity and friction coefficient is shown in Fig. 9. The contour plot presents an ellipse-like shape, so the interaction between die velocity and friction coefficient is obvious (Fig. 9b). Figure 9a is a curved surface; the inhomogeneous deformation reaches the minimum value when the friction coefficient is taken around 0.8 and the velocity is taken around 350 mm/s. From this point to all directions around, the inhomogeneous deformation increases gradually, and the die velocity reaches the minimum value at the coordinates of (0.9,50) and (1.2,50), and the friction coefficient is taken around the two critical values of maximum and minimum. The contours of Fig. 9b show an elliptical shape, and the farther away

Fig. 8 Interaction between temperature and coefficient of friction. **a** 3D plot of temperature—friction coefficient interaction. **b** Contour plot of temperature—friction coefficient interaction
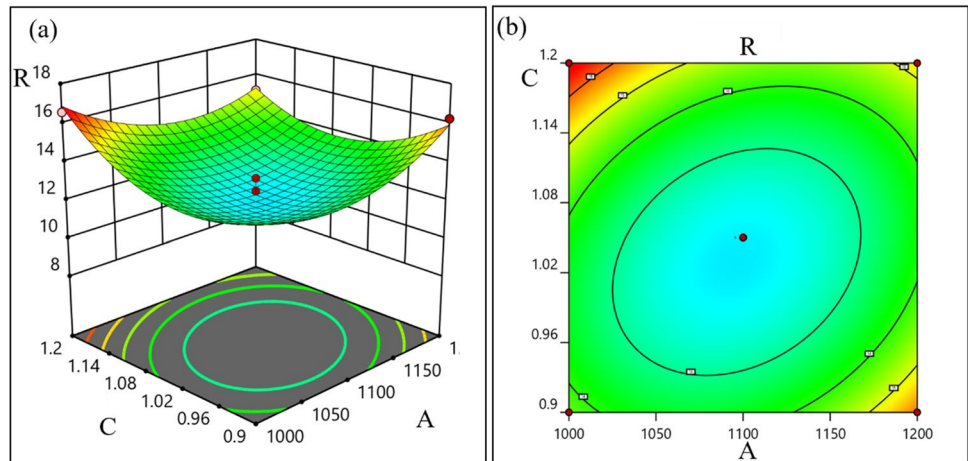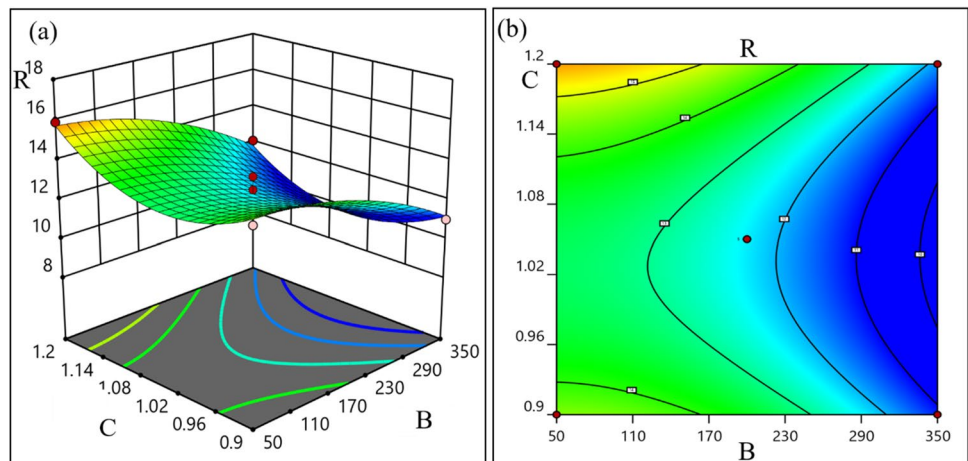

Fig. 9 Interaction between die velocity and coefficient of friction. **a** 3D plot of the interaction between die velocity—friction coefficient. **b** Contour plot of the interaction between die velocity—friction coefficient

from the center ellipse, the denser the contour lines are. This indicates that the inhomogeneous deformation response is not obvious with the change of the two factors: When the die velocity is determined, the inhomogeneous deformation becomes firstly smaller and then larger as the friction coefficient becomes smaller; when the friction coefficient is determined, the inhomogeneous deformation becomes smaller as the temperature increases. Combining Fig. 9a and b, it can be concluded that the inhomogeneous deformation can reach a smaller value when the velocity range is about 350 mm/s and the friction coefficient is about 0.8.

4.3 Determination of optimal parameters for uniform deformation

On the basis of studying the influence law and interaction of various factors, the response surface results were optimized to obtain the best combination of process parameters. When the predicted value of response R reaches the minimum value of 10.934, the temperature is 1240 °C, the mold speed is 336 mm/s, and the friction coefficient is 0.8. According to the optimization scheme, the actual value of the response R can be obtained by repeated simulation. The maximum value of the response R is 9.1. The maximum actual value of the response R is compared with the predicted R, and the error between the predicted value and the actual value of the response R is only 16.7%. The desirability value of the scheme reaches 1.00, and the reliability is high, which verifies the feasibility of verifying the test parameters through the scheme.

5 Microstructure law of cross wedge rolling of gear shaft

Based on the optimal process parameter group obtained, DEFORM-3D software is used to simulate the optimal scheme, in order to refine the grain and obtain the microstructure law of the gear cross wedge rolling. Enhanced

performance of finished gear shafts was verified from a microscopic point of view.

5.1 Selection of feature points

Considering the verifiability of the subsequent experiments, the special positions of the tooth profile, the axle center, the axle edge of the first stepped shaft, the axle center, and the axle edge of the second stepped shaft were selected and labeled as 1–7. The selected positions are shown in Fig. 10. Positions' microstructural evolution at different sections of wedge cross rolling forming is analyzed separately.

5.2 Analysis of microstructure simulation results

5.2.1 Tooth microstructure simulation analysis

When the blank is not in rolling, the grain and boundary of the wedge section are shown in Fig. 11. It can be seen from the figure that the grain size of the tooth top 1, tooth profile 2, and tooth root 3 shows a general trend: the grain from the boundary continues to refine and grow, and the final formation of the grain is smaller than the original grain. Before rolling, the blank is preheated by high temperature and stabilized above 1200 ℃; the system is in an unstable state. When placing the blank on the mill and the die starts to wedge into the blank, with the depth of the wedge section, the blank deformation increases, dislocation density continues to increase, and the internal deformation savings energy gradually increased; the system is in an extremely unstable high-energy state. When the deformation amount reaches a certain degree, dynamic recrystallization occurs. From Fig. 11b to d, it can be seen that new nuclei begin to grow at the boundary of the grains, and the new nuclei are fully grown, but the new grains that grow into the new grains are still smaller than the original grains, and it is believed that the grains are refined in this process.

The grain changes at different forming sections at tooth profile 2 are shown in Fig. 12. Comparing Fig. 12a with Fig. 11, it can be seen that in a short period of time, the

Fig. 10 Position selection for microstructure simulation
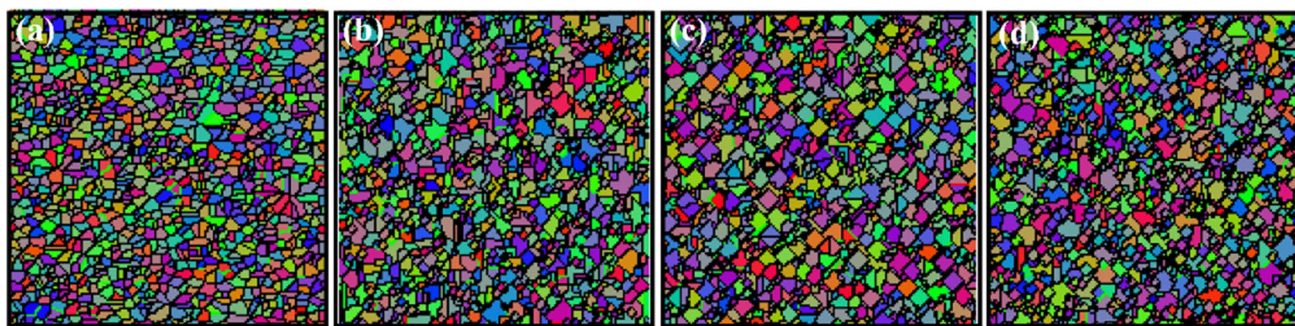

Second step shaft

First step shaft
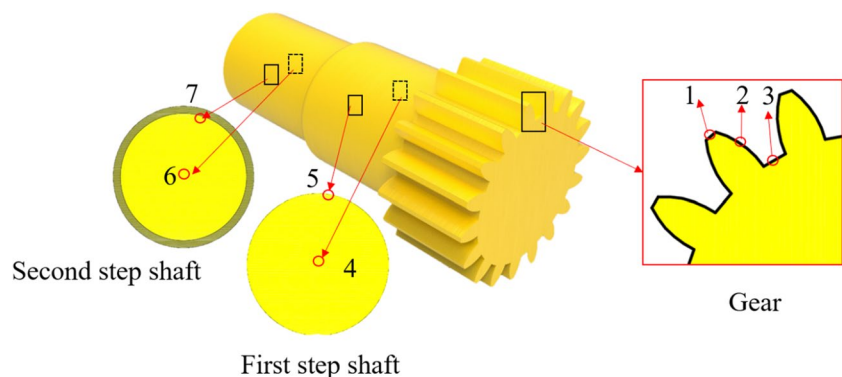
Gear

Fig. 11 Grain and boundary diagram of the teeth in the wedge-in section of the rolled work **a** pre-roll, **b** pre-wedge, **c** mid-wedge, **d** post-wedge
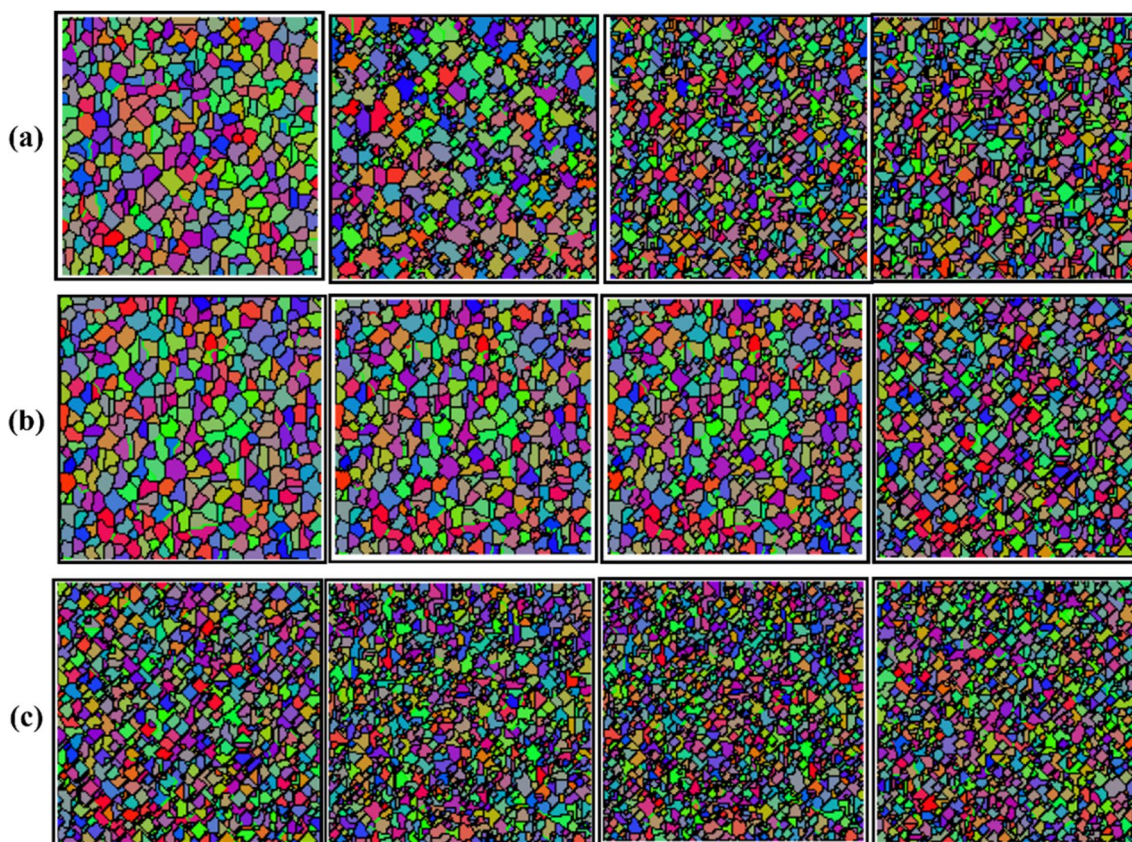

Fig. 12 Grain variation at tooth profile section of the gear. **a** Feed section. **b** Finishing section. **c** After finishing section

grains are growing, but there is a general trend of refinement. Starting from the finishing section, including the section after the finishing section, the grain at each section is significantly refined compared with the previous grain. The partially enlarged view of the toothed profile position is shown in Fig. 13, in the feeding section and the finishing section, because the die starts to contact the blank rolled work over a large area and to extrudes, a larger and more pronounced strain area is formed in the toothed work, resulting in the dynamic recrystallization behavior occurring significantly.

5.2.2 Analysis of shaft microstructure simulation results

The microstructure grain and boundary simulation process of the first-step shaft at the position of axis 4 is shown in Fig. 14; it can be seen from the figure that the overall grain refinement trend is basically the same as that of the tooth work, and there is a tendency for the grain to grow up in the latter section, and there is a fluctuation in the grain size, but as a whole, the grain in the latter section is much smaller than that in the initial section. The degree of grain
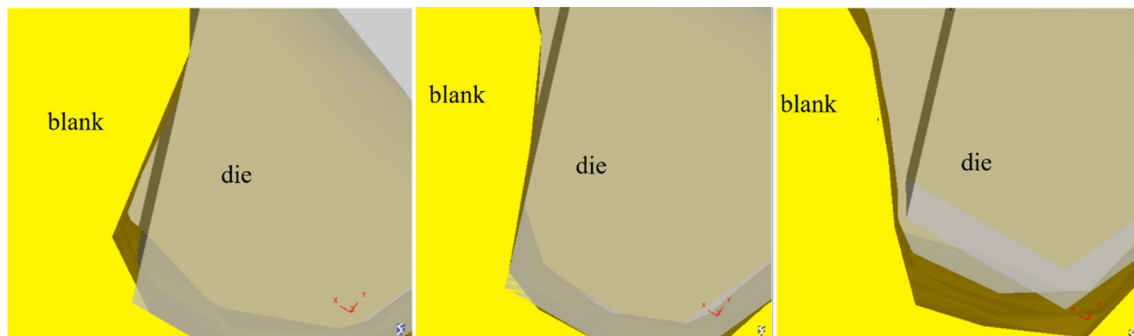
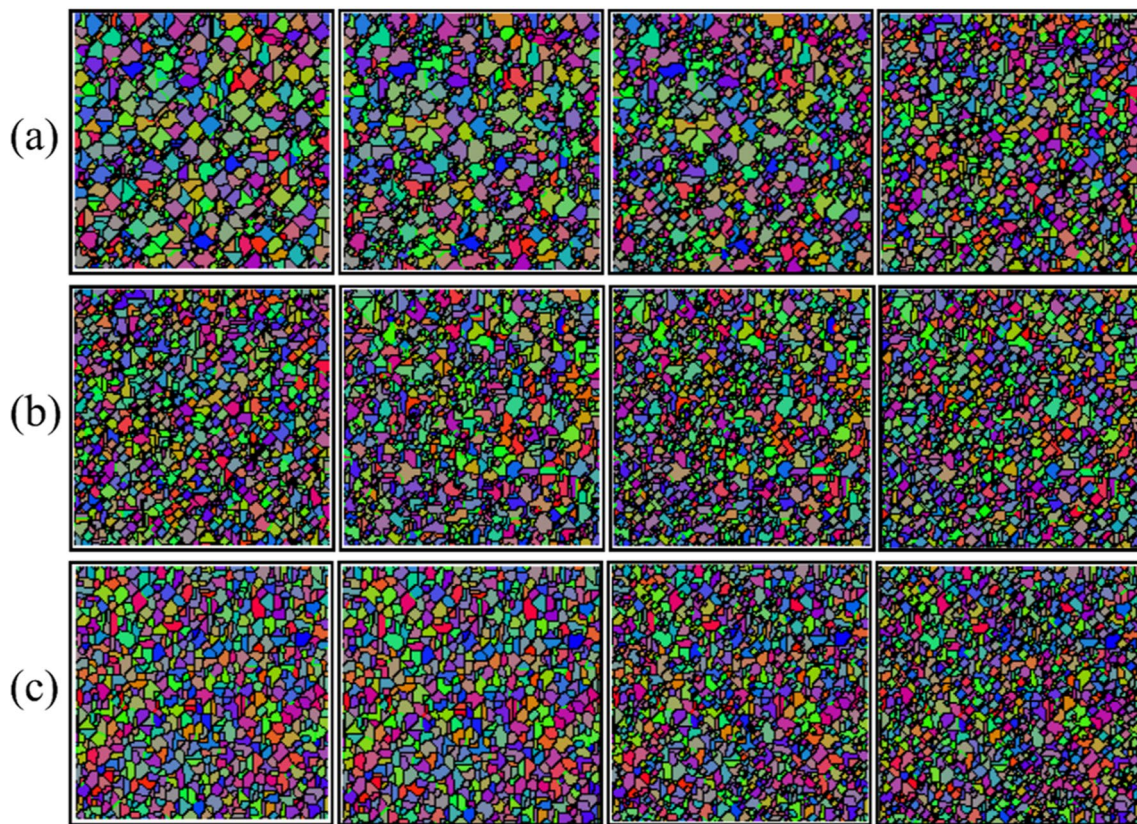**Fig. 13** Partial enlargement at the location of the tooth formation

Fig. 14 Simulation process of the microstructure grain and boundary at the axial position of the first stepped shaft. **a** The first wedge segment. **b** The first spreading segment. **c** After the first spreading segment

refinement in the axial part is higher than that in the tooth part, and the behavior of generating new grains from the grain boundary is more obvious, and the degree of grain growth and refinement iteration is more intense; this is a result of the deformation and temperature factors; on the one hand, the larger deformation areas in the tooth section are generated only at the tooth formation, so the degree of deformation in the shaft section is much higher than that in the tooth section; on the other hand, the shaft is in more

frequent contact with the die, the contact area is larger, and the temperature change is more obvious, which results in more significant temperature variations.

In the recrystallization period, on the one hand, the nucleus is in the non-stop growth. While the nucleus is growing, the rolled work is undergoing a lot of metal deformation. Before the completion of recrystallization, if the dislocation density in the center's grain reaches another recrystallization, then a new cycle will start again. So, the

Fig. 15 Comparison of grains and boundaries at axial center and those at axial edge of the first broadening section. **a** Axial center. **b** Axial edge
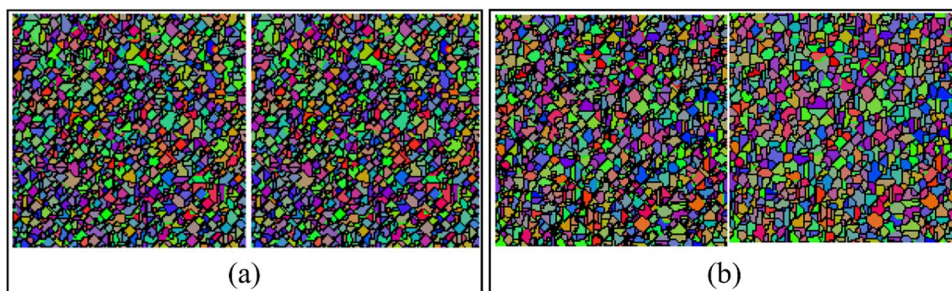
new grains begin to grow again. Therefore, in the rolled piece deformation process, the grain changes show a cyclic change.

Grain variations at the axial center and axial edges are shown in Fig. 15. In the initial section, the difference in grain size between the axial edge and the axial core is not significant, but as the section progresses, the axial edge grain refinement is weaker than the axial core, resulting in the edge of the axial grains larger than the axis at the grains. The reasons are the degree of deformation and temperature; on the one hand, the shaft edge is in contact with the die and air, and the temperature of the shaft edge is lower than that in the shaft's center; on the other hand, as the amount of pressure into the die, the deformation of the shaft edge in the axial direction is much larger than the deformation of the shaft center. Under the combined effect of the temperature and metal deformation, the above situation has arisen.

6 Experiment on cross wedge rolling of gear shaft

6.1 Material selection

The experimental material used is No. 45 steel. No. 45 steel has high strength and possesses plasticity and toughness. It is widely used in various fields such as mechanical works, and is also the most common material selected for shaft works processing. The primary blank is shown in Fig. 16, and the finished rolled product is shown in Fig. 17.

6.2 Analysis of forming quality in appearance

The number of teeth of the gear was observed, and the number of teeth was 18, and the tooth shape was relatively uniform, without the phenomenon of chaotic teeth. Common normal, the whole depth of tooth, and tip addendum were measured, comparing experimental values, simulated values, and theoretical values. Specific values as shown in Fig. 18: the absolute error between the actual value and the theoretical value of the common normal is within 0.5 mm, the relative error is within 10%, and its simulated values
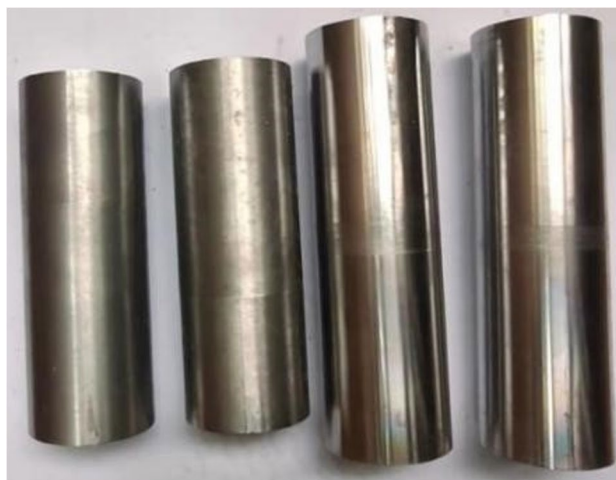

Fig. 16 The primary blanks

Fig. 17 Finished product of the cross wedge rolling experiment

are in perfect match with the theoretical ones, indicating that the individual gear rolling is relatively uniform. The error of average the whole depth of tooth, average tooth length, and average tip diameter are all controlled within 10%, of which the error of tip diameter and gear length is within 5%, indicating that the optimization results of gear formation quality are good, and the quality of tooth formation is improved significantly.

Fig. 18 Comparison of teeth values
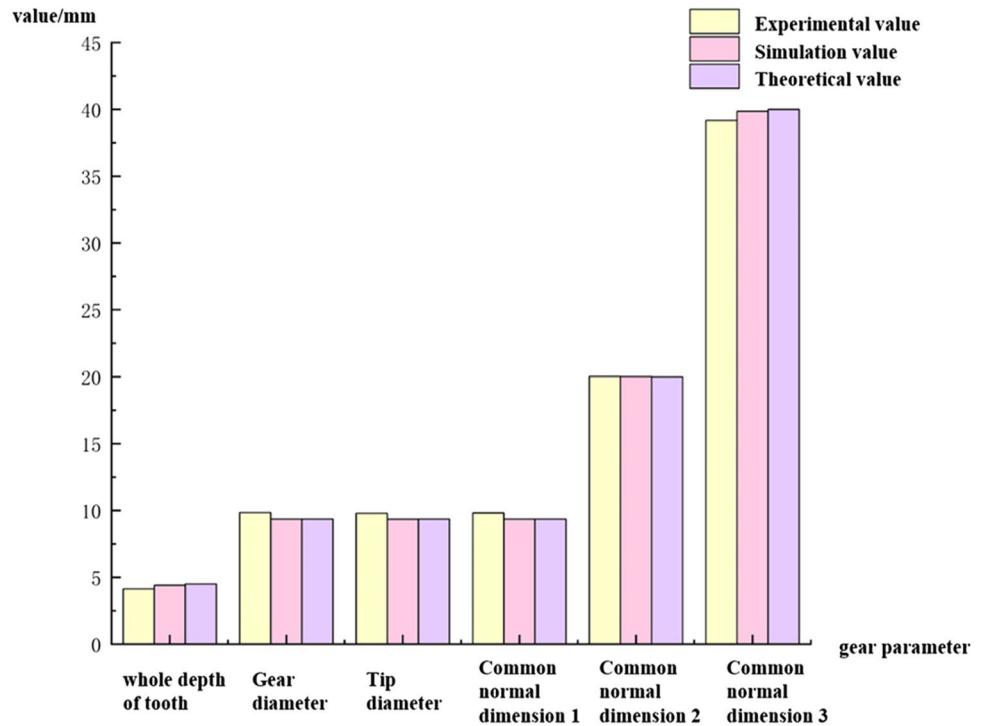
Shaft's diameter is measured from five different positions in a circle and takes the average value; the length of the rolled work is divided into five axial segments, and each axial segment is measured five times and takes the average value. Measure the stepped shaft's data, the specific values are shown in Fig. 19. The figure shows that the stepped

Fig. 19 Comparison of axis values
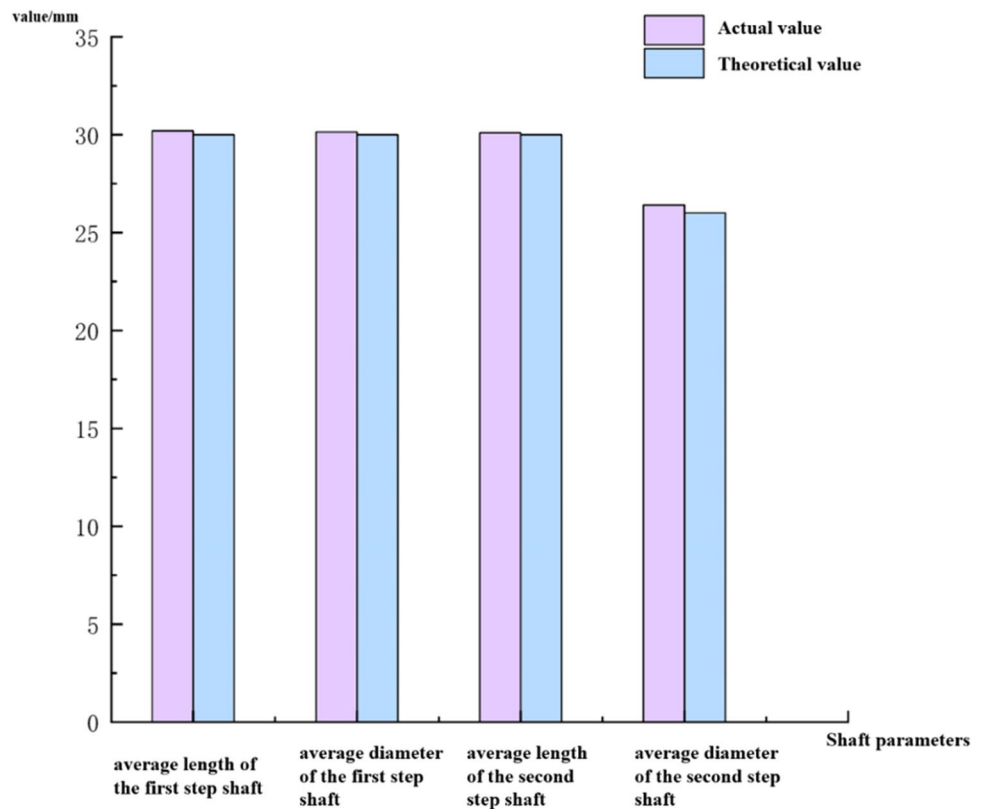
shaft's relative error between the actual dimensions and theoretical dimensions is less than 2%, which is small and meets the requirements.

6.3 Analysis of microstructure results

Five points on the rolled work were selected for grain size inspection as shown in Fig. 12; five points are selected for grain size testing; the 8 mm×8 mm×3 mm cubic specimen is cut on the axial side of the first and second stepped shafts, and 10 mm×10 mm×3 mm cubic specimen were cut on the axial center. Since the teeth are small enough to be cut in pieces, the teeth are cut as a whole specimen, and the tooth

Fig. 20 Tongue in groove diagram

shape as well as the tooth center are observed separately. The cut metal blocks inlay are shown in Fig. 20.

The inlays were placed in an etching solution at 70 °C, and when the detection area has darkened, remove it, then polished gently on a polishing cloth for 1–4 s. The treated specimens were placed under a microscope for observation. The observation diagrams of each position are shown in Fig. 21. It can be seen in the figure that the degree of grain refinement in the shaft work is obviously higher than that in the tooth work, and the degree of grain refinement in the shaft center is higher than that in the shaft edge. In addition, during the observation of grain microstructure, there is a Weiss organization, because the initial temperature of the rolled piece in the experiment is 1240 ℃; the rolling process was carried out in the cold cooling down, and then quenched after the completion of the rolling; the cooling velocity is too fast resulting in the emergence of Weiss organization. This is consistent with the test conditions.
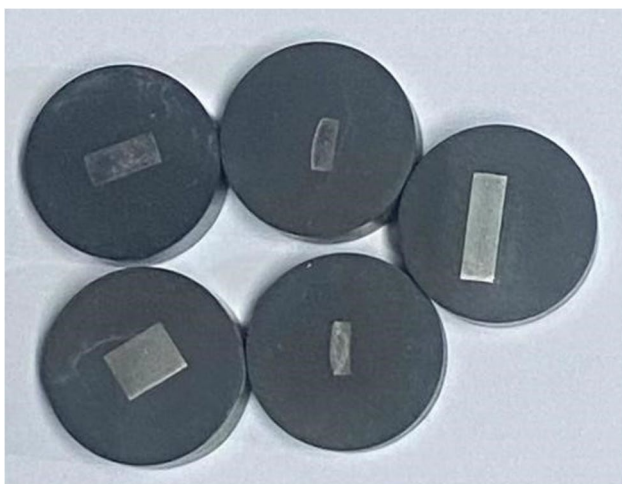
7 Conclusions

(1) The forming of gear shaft by cross wedge rolling consists of five sections. The maximum equivalent strain increases from 3 in the first wedge section to 9.18 in the finishing section. During the rolling and forming process, the strain is mainly concentrated in the contact area between the die and the rolled work, and gradually decreases from the contact area to the end of the shaft.

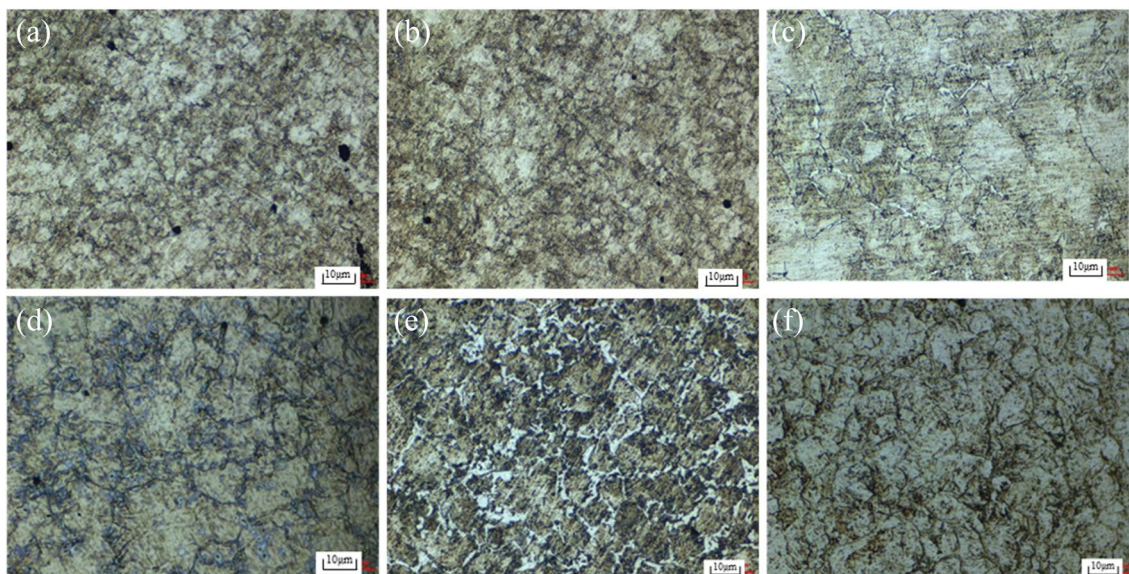(2) The optimal process parameters for cross wedge rolling of the gear shaft are the following: temperature is 1240

Fig. 21 Grain diagram of the finished product. **a** Tooth shape. **b** Tooth center. **c** Shaft center after first section. **d** Shaft edge after first section. **e** Shaft center after second section. **f** Shaft edge after second section

°C, the rotation velocity of the die is 336 mm/s, and the friction coefficient is 0.8. Finite element simulation with this set of parameters yields the smallest inhomogeneous deformation, which is 9.1, and the error between the simulated value and the predicted value is 16.7%. The desirability value of this scheme reaches 1.00, showing that the simulated value can be trusted.

(3) During the rolling process, the tooth grains are continuously refined and grown up from the boundary, and the final formed grains are smaller than the initial grains. The grains of the tooth profile grow in the course of the feeding section. After that, there is a significant refinement of the grains at each of the remaining sections. The grain refinement of the shaft section is higher than that of the tooth section. The degree of grain refinement at the shaft edge is weaker than that at the shaft center, and there is a fluctuation in grain size in the latter sections. The general trend is that the grains in the latter sections are smaller than those in the initial section.

Declarations

Ethics approval This work does not include human and animal; hence, ethical approval from any committee is not required.

Consent to participate This work does not include human and animal; hence, consent to participate in the research is not required.

Consent for publication The authors give the publisher the consent to publish the work.

Conflict of interest The authors declare no competing interests.

References

1. Pater Z (2000) Theoretical and experimental analysis of cross wedge rolling process. Int J Mach Tool Manu 40(1):49–63
2. Yuan WS, Huang RG, Zhang K, Li N, Yang XJ, Wang L (2021) Influence of cross wedge rolling process parameters on hollow shaft rolling formation. China Met Form Equip Manuf Technol 56(02):73–78
3. Yan HJ, Zhang C, Lu HY, Zhang SJ, Zhang JG, Ma SB, Shi XM (2020) Effect of process parameters on thinning and necking of large section multi-step shaft in cross wedge rolling. J Plast Eng 27(9):100–107
4. Han M, Liu JX, Shi MJ, Chen SF, Zhang SH, Chen M (2023) Research on forming of multi-step TC4 asymmetric axis parts by cross wedge rolling. J Ordnance Equip Eng 44(10):57–64
5. Yu ZM, Peng WF, Zhang X, Oleksandr M, Titov V (2022) Evolution of microstructure of aluminum alloy hollow shaft in cross wedge rolling without mandrel. J Cent South Univ 29(03):807–820
6. Zhang Z, Cui SS, Shi XM, Zhang JG, Chen L (2023) Influence of raw material, temperature and guide plate on the quality of wedge rolling products and the way to deal with the situation. Forging & Met Form 05:50–54
7. Pater Z, Tomczak J, Bulzak T, Hua L, Balint D, Lin J, Fiang J (2020) Establishment of a new hybrid fracture criterion for cross wedee rolling. Int J Mech Sci 167:105274
8. Pater Z, Tomczak J, Bulzak T (2020) Rapid estimation of ductile crack formation in cross-wedge rolling. J Mater Res Technol 9(6):14360–14371
9. Zeng J (2018) Study on deformation mechanism and application foundation on the cross wedge rolling without end concavity. J Mech Sci Res Inst 2023:12–26
10. Han L, Yu M (2022) The influence of process parameters on head of wedge rolling and their optimization. Yuxi Normal Univ J 38(06):52–60
11. Qu MI, Zheng SH, Wang Y (2022) The influence of diameter reduction on inner hole diameter of step hollow shaft in cross wedge rolling. J Ningbo Univ 35(05):27–33
12. Yan XZ, Liu JP, Ji HC, Wang BY, Zheng ZH, Li Z (2017) Effect of mandrel diameter on the wall thickness uniformity of the hollow valve of 5Cr21Mn9Ni4 by cross-wedge rolling. Chin J Eng 39(02):267–275
13. Huo YM, Huo CL, Ren X, He T, Wang BY, Cui YL, Jia CY, Liu KR, Du XY (2023) Numerical prediction of microstructure evolution of high-speed railway axle formed using hot cross wedge rolling. Mater Today Commun 35:105985
14. Feng P, Yang CP, Wang BY, Li JL, Liu R (2021) Microstructure and mechanical properties of TC4 titanium alloy hollow shaft formed by cross wedge rolling. Arch Civ Mech Eng 21(3):129
15. Xia YX, Shu XD, Zhu DB, Pater Z, Bartnicki J (2021) Effect of process parameters on microscopic uniformity of cross wedge rolling of GH4169 alloy shaft. J Manuf Process 66(10):145–152
16. Xu Q, Zhao AL, Chen ZG, Hu JL, Chen MZ, Hu HP (2022) Research on the influence of process parameters of titanium alloy cross wedge rolling on the evolution law of microstructure. Mod Ind Econ Inf 12(05):232–234
17. Chen XG, Shu XD, Lian QJ (2022) Effect of feed rate on forming quality of cross wedge rolling of gear shaft teeth. Metalurgija 61(3–4):713–716
18. Xu CL (2013) Three-dimensional finite element simulation of wedge cross rolling involute gear axle. Hot Work Technol 42(5):4
19. Xu CL, Wang GD (2013) Study of forming process optimization for involute gear shaft wedge cross rolling. Tuan Ya Chi Shu Forg Stamping Technol 38(1):5
20. Cai HL (2022) Study on the influence of billet temperature on the quality of gear splitting formed by cross wedge rolling of gear shaft. Mod Man Chnol Equip 58(10):94–97
21. Merkel P, Budde L, Grajczak J, Nowroth C, Prasanthan V, Kriwall M et al (2023) Feasibility study for the manufacturing of hybrid

pinion shafts with the cross-wedge rolling process. Int J Mater Form 16(5):4

22. Wei G, Zhang W, Deng Y (2019) Identification and validation of constitutive parameters of 45 steel based on J-C model. Vib Shock 38(05):173–178

23. Wu LD (2012) Study on the quality of tooth profile of involute spur cylindrical gear shaft formed by cross wedge rolling. D. Zhejiang Univ-Sc(07)